Single-Event Analysis of the Packaging of Bacteriophage T7 DNA Concatemers in Vitro

Mao Sun, Donna Louie, and Philip Serwer
Department of Biochemistry, The University of Texas Health Science Center, San Antonio, Texas 78284-7760 USA

ABSTRACT Bacteriophage T7 packages its double-stranded DNA genome in a preformed protein capsid (procapsid). The DNA substrate for packaging is a head-to-tail multimer (concatemer) of the mature 40-kilobase pair genome. Mature genomes are cleaved from the concatemer during packaging. In the present study, fluorescence microscopy is used to observe T7 concatemeric DNA packaging at the level of a single (microscopic) event. Metabolism-dependent cleavage to form several fragments is observed when T7 concatemers are incubated in an extract of T7-infected *Escherichia coli* (in vitro). The following observations indicate that the fragment-producing metabolic event is DNA packaging: 1) most fragments have the hydrodynamic radius (R_H) of bacteriophage particles (±3%) when R_H is determined by analysis of Brownian motion; 2) the fragments also have the fluorescence intensity (I) of bacteriophage particles (±6%); 3) as a fragment forms, a progressive decrease occurs in both R_H and I. The decrease in I follows a pattern expected for intracapsid steric restriction of 4′,6-diamidino-2-phenylindole (DAPI) binding to packaged DNA. The observed in vitro packaging of a concatemer's genomes always occurs in a synchronized cluster. Therefore, the following hypothesis is proposed: the observed packaging of concatemer-associated T7 genomes is cooperative.

INTRODUCTION

Several bacteriophages consist of a double-stranded DNA genome packaged in a protective container (capsid) of protein. Assembly of these double-stranded DNA bacteriophages consists of two independent events. These events are assembly of a DNA-free procapsid and packaging of DNA by the procapsid. The procapsid is also called capsid I in the case of bacteriophage T7. The procapsid changes in several physical characteristics during DNA packaging. The changed T7 capsid is called capsid II. The DNA substrate for packaging is a head-to-tail multimer (concatemer) for both T7 and some other bacteriophages. Mature genomes are cleaved from the concatemer during packaging (reviewed in Casjens, 1985; Feiss, 1986; Serwer, 1989; Fujisawa and Hearing, 1994). In the case of both in vitro (White and Richardson, 1987) and in vivo (Serwer et al., 1992) T7 DNA packaging, a mature right end is formed by cleavage before DNA enters the capsid. The direction of entry is right to left both in vivo (Khan et al., 1995) and in vitro (Son et al., 1993). The left and right halves of T7 DNA are defined by the order of gene expression (Studier and Dunn, 1983). The mature T7 genome has unique ends (nonpermuted genome); the 160 basepairs at the left end are repeated at the right end of the 40-kilobase pair (kbp) T7 genome (Dunn and Studier, 1983).

In the past, the transformations of DNA packaging have been analyzed macroscopically by fractionation of a large population of particles. For example, packaging-associated cleavage of concatemers is observed by pulsed field gel electrophoresis (Son et al., 1988). Averaging causes loss of information during this type of analysis. To avoid this loss of information in the case of in vitro transcription, a single-event analysis has been performed by use of either light microscopy (Schafer et al., 1991; Yin et al., 1994, 1995) or atomic force microscopy (Kasas et al., 1997). This type of single-event analysis also has the potential to overcome limitations of past analyses of T7 DNA packaging.

To perform a single-event analysis of the packaging of concatemer-associated T7 genomes, an appropriate in vitro system is needed. An in vitro system has been developed for the specific packaging of concatemer-associated T7 genomes. This system packages T7 concatemers ~100 times more efficiently than it packages monomeric T7 DNA (Son et al., 1988; Son and Serwer, 1992). The primary component of this in vitro system is one or more lysates of T7-infected cells. The final mixture is called a DNA-metabolizing extract. When DNA is stained with the DNA-specific dye, DAPI (4′,6-diamidino-2-phenylindole), single DNA molecules can be visualized in a T7 DNA-metabolizing extract. Unknown components of the extract dramatically inhibit both photocleavage and photobleaching (Sun et al., 1997). When monomeric T7 DNA is added to a T7 DNA-metabolizing extract, T7 exonuclease causes concatemerization by converting the terminal repeats to single-stranded ends; the single-stranded ends adhere by hydrogen bonding (Son and Serwer, 1992). Fluorescence microscopy of DAPI-stained DNA reveals that the concatemers partition to form an immobile (Brownian motion-free) DNA network. Most segments of the network contain more than one DNA double helix (Sun et al., 1997). After a delay, the network is subsequently cleaved. This cleavage depends on the presence of both a procapsid and two accessory proteins for T7 DNA packaging, p18 and p19 (A T7 protein will be

Received for publication 13 January 1999 and in final form 23 May 1999.
Address reprint requests to Dr. Philip Serwer, Department of Biochemistry, The University of Texas Health Science Center, 7703 Floyd Curl Dr., San Antonio, TX 78284-7760. Tel.: 210-567-3765; Fax: 210-567-6595; E-mail: serwer@uthscsa.edu.

0006-3495/99/09/1627/11 $2.00

labeled by p, followed by the number of the protein's gene from Studier and Dunn, 1983). Thus, the observed cleavage is assumed to be an initiating cleavage of DNA packaging. This cleavage reduces the network to fragments. Assuming that some of these fragments are packageable concatemers, the preconditions have been obtained for performing a single-event analysis of the packaging of concatemer-associated T7 genomes. In the present study we have performed this analysis.

MATERIALS AND METHODS

Bacteriophage and bacterial strains

A bacteriophage protein was selectively eliminated from a DNA-metabolizing extract by use of a polypeptide chain termination (amber) mutation. Both nonmutant T7 (T7wt) and amber mutant T7 are the strains used in Sun et al. (1997). The host for growing amber mutants was *Escherichia coli* 011′. This host suppresses the effects of the amber mutation. The host for T7wt was *E. coli* BB/1. A DNA-metabolizing extract was prepared by infection of *E. coli* BB/1 with an amber mutant (details are in the next section). The mutant gene product is missing from amber mutant-infected *E. coli* BB/1 because this host does not suppress the effects of amber mutations. Amber mutant T7 strains had the following mutant genes (number of gene, followed by function of gene product; reviewed in Studier and Dunn, 1983): 3, debranching endonuclease; 4, primase; 5, DNA polymerase; 6, 5′→3′ exonuclease; 9, scaffolding protein for procapsid assembly; 19, accessory protein for DNA packaging. A T7 amber mutant is named by the numbers of the mutant gene(s) in subscript. For example, $T7_{3,5,6}$ indicates a triple mutant for which the amber mutant genes are 3, 5, and 6. Both T7wt and T7 amber mutants were both grown and purified by use of procedures previously described (Son et al., 1993).

In vitro DNA metabolism

In vitro DNA metabolism was achieved by use of the following procedure. A lysate of T7-infected *E. coli* was prepared by procedures described in Son et al. (1988). The lysate was clarified twice by centrifugation at 2°C, for 5 min, at 60,000 rpm in a Beckman TL-100 tabletop ultracentrifuge. To prepare a DNA-metabolizing extract, the following were added: 19.2 μl clarified lysate, 6.0 μl 50% (w/v) dextran 10,000 (Pharmacia) and 3.3 μl mixture A. The composition of mixture A was 125 μl solution of packaging-stimulators, 6.5 μl DAPI (100 μg/ml), and 1.0 μl β-mercaptoethanol. The solution of packaging stimulators contained 0.1 M $MgSO_4$, 0.02 M ATP, and 0.025 M spermidine, adjusted to a pH of 7.4 with HCl. The DAPI caused <20% inhibition of the in vitro packaging (Sun et al., 1997). To add p6 to an extract missing p6, purified p6 (obtained from United States Biochemicals, Cleveland, OH) was added to a DNA-metabolizing extract (1 part p6 per 10 parts extract) before addition of DNA. To initiate DNA metabolism, a DNA-metabolizing extract was added at 30°C to T7 DNA. The DNA had been purified by phenol extraction of T7wt. The extract/DNA volume ratio was 30:1. The final DNA concentration was 100 μg/ml. Incubation at 30°C in a culture tube was continued until preparation for fluorescence microscopy.

Fluorescence microscopy

To observe metabolizing DNA by fluorescence light microscopy, a DNA-extract mixture was 1) mounted between a cover glass and flat glass slide, and 2) observed at room temperature (23 ± 2°C) by use of procedures previously described. Records were kept on videotape (Sun et al., 1997). Unless otherwise indicated, preparation for microscopy was performed no more than 1 min before observation; the specimen was observed for no more than 3 min before another specimen replaced it. Usually, multiple specimens were prepared from the same DNA-extract mixture during the process of incubation of this mixture at 30°C. The use of multiple specimens was made because of loss of activity during observation. However, the DNA-metabolizing extract inhibits photobleaching and photocleavage of DNA (Sun et al., 1997).

When indicated, the above procedure of fluorescence microscopy was modified to observe DNA metabolism initiated at a lower temperature. The following are the modifications: 1) after addition of DNA to a DNA-metabolizing extract, the extract was kept at 0°C for 30 min before preparing a specimen for light microscopy. Concatemerization, but not packaging, occurs at 0°C (Son et al., 1988). 2) After 30 min at 0°C, a specimen was prepared with a cover glass and flat microscope slide that were pre-chilled to 0°C. After preparation, the specimen was allowed to gradually warm to room temperature while on the specimen stage. 3) The DNA-metabolizing extract had been clarified by use of a single centrifugation. This modified procedure will be called the low temperature procedure.

Characterization of DNA molecules by light microscopy

The resolution of fluorescence microscopy is not sufficient to reveal internal detail for most conformations achieved by a randomly coiled monomeric T7 DNA molecule. The image is usually a symmetrically broadened point of light (Smith and Bendich, 1990; Sun et al., 1997). As the DNA becomes longer, an asymmetrical appearance becomes more probable at any given time. However, the time-averaged appearance is symmetrical (Serwer et al., 1995). Nonetheless, single DNA-containing particles can be characterized by quantifying either total fluorescence intensity (I) or Brownian motion. Unpackaged DNA can be discriminated from packaged DNA. The following characterizations are performed here:

First, the effective hydrodynamic radius (R_H) was determined by quantifying the Brownian motion. To determine R_H, initially the mean-square displacement along the x axis ($\langle \Delta x^2 \rangle$) was determined in a fixed time interval, Δt, from digitized videotaped images (TDK, Hi-Fi, extra high grade videotape). Procedures of data analysis are described in Griess et al. (1993). The error in Δt from stretching of the videotape was <1%. For all experiments, $\Delta t = 0.2$ s. Subsequently, the following relationship (Perrin, 1913; Chapter 6 in Tinoco et al., 1995) was used:

$$R_H = kT\Delta t/(3\pi\eta\langle \Delta x^2 \rangle) \quad (1)$$

where T is the absolute temperature, k is the Boltzmann constant, and η is the viscosity of the DNA-metabolizing extract. The value of η was determined by quantifying the Brownian motion of a spherical standard of known R_H (microscopic viscometry). The standard was a latex sphere that stained with DAPI. The manufacturer's radius was 30 nm (Polysciences, Warrenton, PA). Quantification of the Brownian motion of this sphere yielded an R_H of 28.7 ± 1.0 nm. The suspending solution was a DNA-metabolizing extract without a lysate. The η of this solution had been determined with an Ostwald viscometer (Chapter 10 in Bull, 1971). The latter value of R_H was used here. Analysis of sedimentation coefficients yields the conclusion that R_H is related to the length of the DNA double helix, L, by Bloomfield et al. (1974, p. 218):

$$R_H = 2.71 \times L^{0.5} \text{ (length in nm)} \quad (2)$$

That is, R_H for the 40-kbp monomeric T7 DNA is predicted to be 316 nm. By low-angle x-ray scattering, the R_H of mature bacteriophage T7 is 30.1 nm (Stroud et al., 1981). The exponent of Eq. 2 has also been found to be 0.6 (Smith et al., 1996).

The mean value of Δx never deviated significantly from 0 (i.e., no detectable drift occurred) during determination of $\langle \Delta x^2 \rangle$. The same observation was made for displacements in the orthogonal direction. Thus, displacements in two orthogonal directions were combined to determine R_H. The experimental error is dominated by sampling error for values of R_H in Fig. 4, *a–d*. Forty displacements in a 4-s time interval were measured for each R_H value in Fig. 4; error bars are in the figure. All other measurements of R_H use a minimum of 1000 displacements. Measurements of η by microscopic viscometry use 500 displacements obtained in a 4-s time

interval. The total time of incubation of the DNA-extract mixture, both before and during microscopy, is the indicated time at which measurement of η was made.

Second, the L of a DNA molecule was determined from I by assuming that L was proportional to I (Schwartz et al., 1993). The constant of proportionality was determined by measuring the I value of monomeric T7 DNA. The value of I on an arbitrary scale was determined from the density of a videotaped image. This density was determined by densitometry and corrected for nonlinearity. Procedures have been previously described (Sun et al., 1997). Brownian motion causes variable defocus of the particles observed here. Thus, the I value of a particle's brightest image in a 0.5-s time span was assumed to be the I value of that time span. That is, the I of the brightest image was assumed to be the I at focus. Comparison of I values from two different specimens was performed by microscopy of one specimen immediately after microscopy of the other, without changing instrumental settings. When determined in a $T7_{3,5,6}$ DNA-metabolizing extract, the I value of phenol-extracted mature T7 DNA was 3.1 ± 0.2 times as great as the I value of the same DNA packaged in a bacteriophage particle. When determined in the extract's buffer without the extract, this ratio was 1.5 ± 0.1. This latter value has been confirmed by conventional fluorometry. The reason for this difference in ratio is not known.

RESULTS

Verification of the cleavage that initiates DNA packaging

DNA excised from in vitro T7 DNA networks has already experienced an initiating cleavage of DNA packaging (see Introduction). This DNA potentially will undergo packaging that might be visualized by fluorescence light microscopy. Thus, the excised DNA was monitored in packaging-competent extracts. Attempts were made to find packaging-like transformations of concatemer-sized DNA molecules. The activity of a DNA-metabolizing extract was tested by determining η as a function of time after the start of incubation with DNA. This procedure is more efficient than the previously used (Sun et al., 1997) procedure, quantification of cleavage events observed directly by fluorescence microscopy. Formation of concatemers in both a $T7_3$ extract (missing p3 DNA debranching endonuclease only) and a $T7_{3,19}$ extract (missing both p3 and the p19 accessory protein for DNA packaging) caused an initial increase in η (Fig. 1; plots are labeled by the extract used). This increase in η was accompanied by formation of the immobile DNA network (images not shown). In the case of the $T7_3$ extract, the increase in η was followed by a network disintegration-associated decrease in η to a level within 15% of the η of the DNA-extract mixture before concatemerization (Fig. 1). In contrast, η continued to increase in the case of the $T7_{3,19}$ extract (Fig. 1). Thus, the decrease in η in the $T7_3$ extract was caused by initiation of DNA packaging, not by a nonspecific nuclease. The behavior of the $T7_3$ extract was mimicked by either a p6-supplemented $T7_{3,5,6}$ extract or a $T7_{3,5}$ extract (data not shown). These latter three extracts will be used interchangeably.

The fragments released by p19-induced cleavage of the DNA network were of two types: 1) most observed fragments were small enough to undergo perceptible Brownian motion (Fig. 2 *a*). 2) Other fragments were much larger and more irregular. These latter fragments had the appearance of

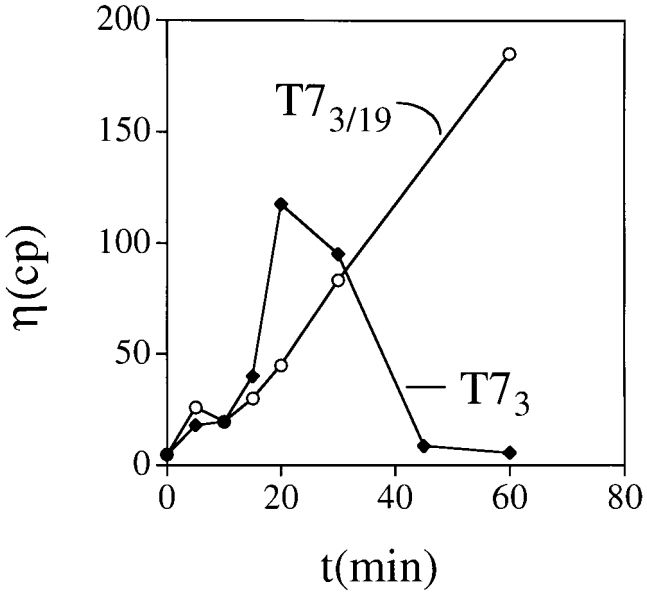

FIGURE 1 Viscosity as a function of time during in vitro DNA packaging. After adding T7 DNA to a DNA-metabolizing extract, η was determined as a function of time at 30°C. Microscopic viscometry was used. The DNA-metabolizing extract used is indicated in the figure.

an aggregate (aggregate-like particle; Fig. 2 *b*). Review of videotapes revealed that aggregate-like particles were formed by collapse of a segment of the DNA network during cleavage. Review of videotapes also revealed no formation of aggregate-like particles by aggregation of smaller fragments. This observation agrees with the absence of any aggregate-like particle in DNA-metabolizing extracts that do not form a network (i.e., extracts without p6 exonuclease; Sun et al., 1997). Aggregate-like particles were not noted in Sun et al. (1997). Subsequent review of the videotapes of that previous study confirmed the presence of the aggregate-like particles after cleavage of the DNA network. The I value of the aggregate-like particles was usually so high that it could not be measured. The approximate mass of small (diffusing) particles per area indicates that most DNA has become part of aggregate-like particles after disintegration of the network. The percentage of DNA not in aggregate-like particles was 5–20%, depending on the field. This percentage was raised to 20–40% when p3 was present (in a $T7_5$ DNA-metabolizing extract, for example; data not shown). A known activity of p3 is debranching endonuclease (reviewed in Studier and Dunn, 1983). Thus, the aggregate-like particles appear to be regions of the DNA network that had a comparatively high density of branches. Intracellular T7 DNA apparently resembles the in vitro T7 DNA network in forming a multigenomic complex in which branched DNA is physically separate from concatemeric DNA (Serwer, 1974).

Characteristics of potential substrates for DNA packaging

Before monitoring to find DNA packaging-like events, potential substrates for DNA packaging were characterized.

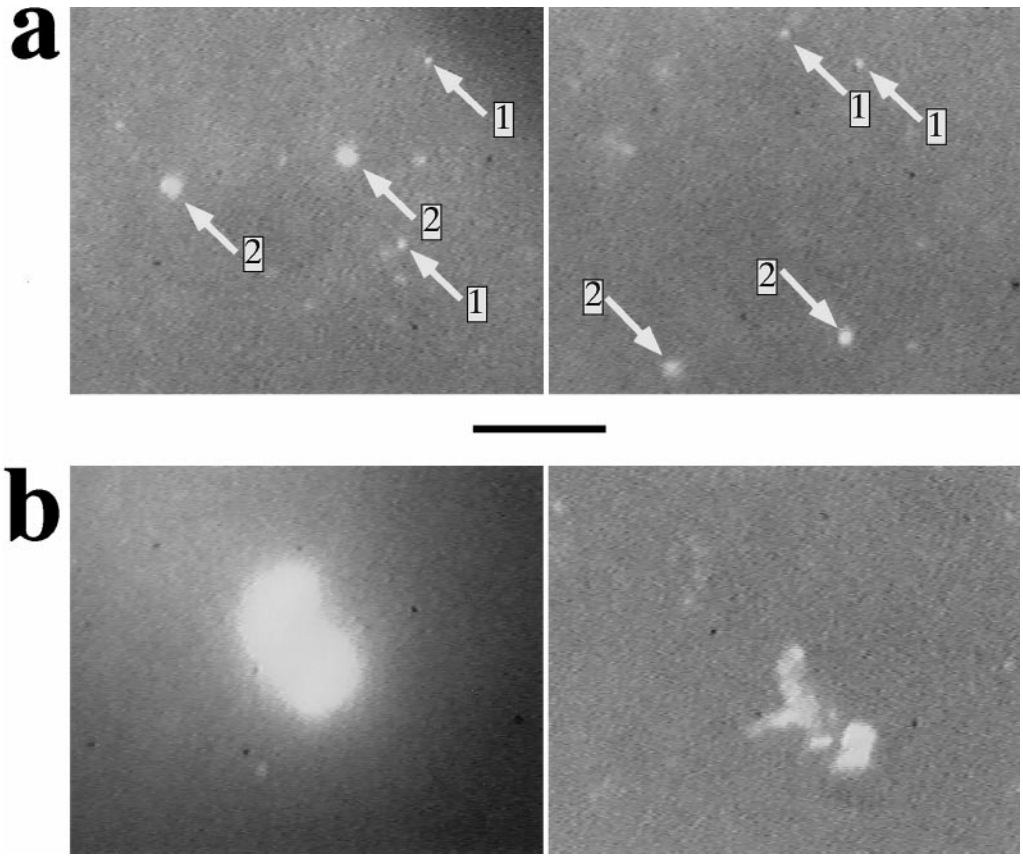

FIGURE 2 DNAs cleaved from a DNA network. After adding T7 DNA to a $T7_{3,5}$ DNA-metabolizing extract, incubation was performed at 30°C. The DNA-extract mixture was observed by fluorescence microscopy at 60 min after the start of incubation. (*a*) Fields that contain particles most of which appear to be single DNA molecules. (*b*) Fields that contain aggregate-like particles. The length of the bar is 10 μm.

The smaller cleavage products of a $T7_{3,5}$ DNA-metabolizing extract appeared to be in two classes: 1) most had a comparatively low *I* value that was comparatively invariable (indicated by *arrows 1* in Fig. 2 *a*). 2) Others had a higher, more variable *I* value (indicated by *arrows 2* in Fig. 2 *a*). All class 1 and class 2 DNAs underwent Brownian motion. The number of type 1 DNA molecules was 2–4 times the number of type 2 DNA molecules at 45 min after the start of incubation. This ratio increased to 10–15 at 60 min. All class 1 and some, but not all, class 2 DNAs had a time-averaged symmetrical appearance. This symmetrical appearance suggests that these latter class 2 DNAs are not aggregates; they will be assumed to be single DNA molecules. Previous analysis by pulsed field agarose gel electrophoresis (Sun et al., 1997) reveals most DNA molecules to have the length of monomeric T7 DNA at 30–60 min after the start of incubation at 30°C. This electrophoretic analysis suggests the hypothesis that class 1 DNA cleavage products have the length of mature T7 DNA. To test this hypothesis, R_H was determined for class 1 DNA cleavage products. This R_H was compared to the R_H for mature T7 DNA molecules added to an unsupplemented $T7_{3,5,6}$ DNA-metabolizing extract. Because the $T7_{3,5,6}$ extract had no p6, this extract did not concatemerize DNA. The endogenous, class 1 DNA cleavage products had a mean $R_H = 164$ nm; the exogenous mature T7 DNA molecules had a mean $R_H = 148$ nm (Table 1). Thus, the endogenous, class 1 DNA molecules do appear to be approximately mature-length T7 DNA. However, R_H was about one-half the R_H predicted by Eq. 2. Comparison with R_H values in buffer (0.1 M NaCl, 0.01 M sodium phosphate, pH 7.4, 0.001 M EDTA; η determined with an Ostwald viscometer) revealed that most of this difference in

TABLE 1 R_H values

Specimen*	R_H (nm)
Class 1 DNA	164 ± 6
Class 2 DNA (mean) value	310
Class 2 DNA (individual) values	328, 328, 461, 285, 262, 303, 260, 244, 236, 315, 261, 307, 402, 399, 306
T7 DNA	148 ± 6
High mobility fragments	30.9 ± 1.0#
Bacteriophage	29.4 ± 1.0

R_H values were determined by procedures described in the Materials and Methods section.

*The specimens are the following: class 1 and class 2 DNA, DNA molecules defined in the text. T7 DNA, monomeric T7 DNA in an unsupplemented $T7_{3,5,6}$ DNA-metabolizing extract. Bacteriophage, intact particles of bacteriophage T7 in a $T7_{3,5,6}$ DNA-metabolizing extract. High mobility fragments, fragments described in the text.

#The result is the average for 25 high mobility fragments.

R_H values was caused by the presence of the DNA-metabolizing extract. That is, the DNA-metabolizing extract has caused compaction of (unpackaged) monomeric T7 DNA. The extent of this compaction is at least twofold less than the compaction that the spermidine of the DNA-metabolizing extract would induce without the other constituents of the extract (Takahashi et al., 1997).

Analysis of R_H for each of 15 randomly selected class 2 DNA molecules revealed that all were longer than mature-length T7 DNA (Table 1). If the $R_H \propto L^{0.5}$ feature of Eq. 2 is used, then the R_H of the class 2 DNA molecules in Table 1 implies L values between 2 and 8 times the L of mature T7 DNA.

Visualization of DNA packaging-like transformations of class 2 DNA molecules

Monitoring of randomly videotaped fields revealed that most class 1 and class 2 DNA molecules in T7 DNA-metabolizing extracts underwent no visible internal transformations. This observation is not surprising even if all molecules eventually did undergo a metabolic transformation. The reason is that the period of observation is but a "snapshot" of the total time in which metabolism occurs. However, occasionally a class 2, but never a class 1, DNA molecule formed several grape cluster-like lobes. An example is the class 2 DNA molecule indicated by an arrow in both the first and last frame of Fig. 3; a p6-supplemented $T7_{3,5,6}$ extract was used. In Fig. 3, the time (s) of a frame is indicated in the upper left corner; time = 0 is chosen at the beginning of observation. In lobe-forming class 2 DNA molecules, each lobe underwent Brownian motion that appeared independent of the Brownian motion of the other lobes (0–26-s frames in Fig. 3). After the formation of lobes, the Brownian motion of the lobes visibly increased as time increased. Eventually, the lobes separated from each other as though cleavage had occurred between them (28–30-s frames in Fig. 3). Qualitatively, no evidence was observed for time-averaged drawing together of the lobes at any point in this process. The separated products of cleav-

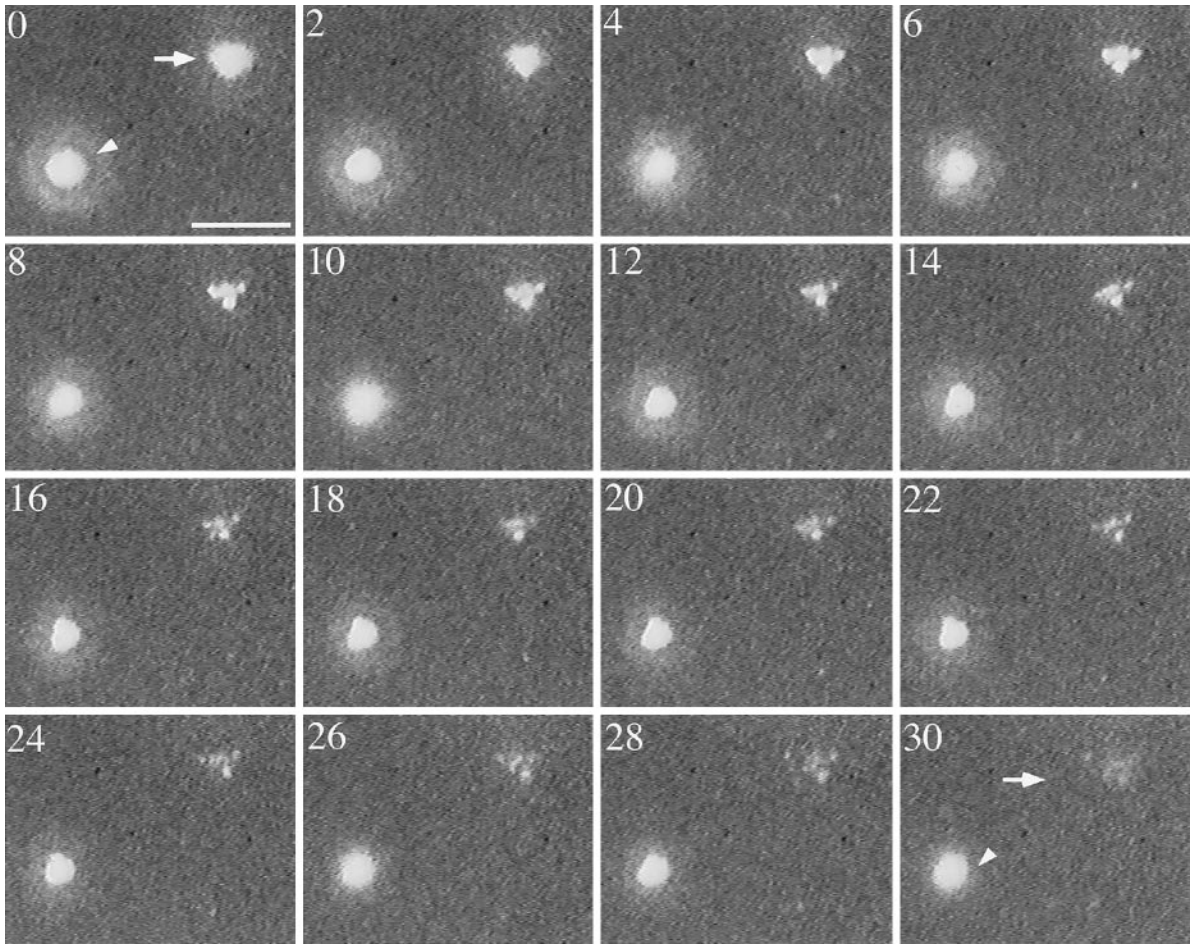

FIGURE 3 DNA packaging-like event of a class 2 DNA molecule. T7 DNA was added to a p6-supplemented $T7_{3,5,6}$ DNA-metabolizing extract. Fluorescence microscopy was performed after incubation for 60 min. In a search for internal transformations of concatemers, videotaped images were reviewed. An active class 2 DNA molecule is indicated by an arrow in the first and last frames (time (s) is indicated at the *upper left*). As described in the text, changes in this molecule are observed in intermediate frames. An inactive class 2 DNA molecule is indicated by an arrowhead in the first and last frames. The length of the bar is 10 μm.

age will be called high mobility fragments. When a class 2 DNA molecule underwent clustered, multiple cleavages, neighboring class 2 DNAs of comparable I values (for example, the DNA indicated by an arrowhead in Fig. 3) underwent no perceptible cleavage. Illumination for an additional time as long as 90 s did not cause cleavage. Thus, random photolytic cleavage is assumed not to be the cause of the observed fragmentation of class 2 DNA molecules. Evidence presented below indicates that high mobility fragments are T7 capsids that have packaged DNA.

To further test for randomness of observed cleavage, videotapes were comprehensively screened for cleavage events in a $T7_{3,5}$ DNA-metabolizing extract. The videotaped fields are assumed to be random because cleavage was never noticed during videotaping. No fewer than five high mobility fragments were produced by all class 2 DNA molecules that 1) underwent at least one observed cleavage event and 2) were continuously observed for at least 20–25 s before production of high mobility fragments (15 class 2 DNA molecules, total). In all cases, clustering in time caused the appearance of a grape-like cluster in space. The clusters were similar to the cluster of Fig. 3. Neighboring, illuminated class 2 DNA molecules did not undergo either lobe formation or any other visible transformation. Class 1 DNA molecules were never cleaved. The clustered cleavage is not a random nonspecific cleavage because clustering occurs in the absence of cleavage of most DNAs. In addition to being nonrandom, the observed cleavages were completely inhibited by fluorescence microscopy performed for 90 s. The cleavages were not inhibited by incubation without preparation for microscopy. Thus, the observed fragmentation occurred via metabolism inhibited by the conditions of microscopy.

The frequency of multilobed DNA molecules was also determined without considering whether high mobility fragments were subsequently produced. The multilobed molecules were 1–3% of all DNA molecules (class 1 and class 2) observed during random screening of fields at 45 min after the start of incubation. This number increased to 3–7% at 60 min. At 60 min, roughly 50% of the multilobed molecules eventually underwent formation of high mobility fragments. The number of lobes in the remaining (inert) multilobed DNA molecules was difficult to count. However, about half the inert multilobed DNA molecules appeared to have two to four lobes, rather than five or more. Apparently, the probability of the lobe $\rightarrow$ high mobility fragment transformation increased as the number of lobes increased. The precursor of a multilobed DNA molecule always had time-averaged symmetry when observed both before and after the formation of lobes.

Characterization of high mobility fragments

To help identify the high mobility fragments, the R_H of these fragments was determined. R_H was determined by measuring $\langle \Delta x^2 \rangle$ and using Eq. 1. The value of η was determined by microscopic viscometry. To minimize time-dependent change in η, the time of observation was 45–60 min after the start of incubation (Fig. 1). The average R_H for high mobility fragments was found to be 30.9 ± 1.0 nm for one class 2 DNA molecule (see Fig. 4 *a*, below). This R_H is not significantly different from the x-ray scattering-determined radius of bacteriophage T7, 30.1 ± 0.2 nm (Stroud et al., 1981). Results for several other class 2 DNA molecules were similar; the results averaged for all high mobility fragments are in Table 1. Further details are described in the next section.

In addition to having the R_H of bacteriophage T7 particles, the high mobility fragments also had the I values of bacteriophage particles produced in a DNA-metabolizing extract ($\pm 6\%$). I was measured by the procedures of the Materials and Methods. High mobility fragments are found only in DNA-metabolizing extracts that are competent to package DNA. Thus, the conclusion is drawn that the high mobility fragments are DNA-containing T7 capsids. These capsids may be missing comparatively small bacteriophage components such as the short T7 tail (see Steven and Trus, 1986). The values of I indicate that a mature genome's amount of DNA ($\pm 6\%$) is present.

Characterization of lobes

To characterize lobes of class 2 DNA molecules, the R_H of each lobe was separately determined. The time of observation was 45–60 min after the start of incubation. The basis for selection of class 2 DNA molecules was the presence of lobes that could, by chance, be continuously tracked for the greatest time before diffusion out of focus. Lobes-high mobility fragments diffused out of focus in a pattern that appeared random. An R_H versus time plot is shown in Fig. 4 *a* for all six lobes observed in one class 2 DNA molecule in a $T7_{3,5}$ DNA-metabolizing extract. The time = 0 point was obtained from the first frame videotaped. Lobe formation was not discerned during the process of videotaping. Thus, the initial phases of lobe formation were not observed for either the type 2 DNA molecule of Fig. 4 *a* or any other type 2 DNA molecule. However, the initial phases of lobe formation were observed in low temperature preparations (next section). As time increased in Fig. 4 *a*, all six lobes underwent a monotonic decrease in R_H. When a lobe became a high mobility fragment, the R_H was indistinguishable from the R_H of bacteriophage T7, 30.1 nm. No evidence was obtained for the production of unpackaged T7 genomes during the formation of high mobility fragments. Fig. 4 *a* reveals that the various lobes did not achieve minimum R_H values at the same time. The lower plot achieved a minimum R_H value 10–15 s before the upper plot did the same. However, this spread in time is small in comparison with the range of times in which the DNA-metabolizing extract remained active in packaging concatemer-associated T7 genomes, ~30 min. Thus, the conclusion is drawn that clustering in space is a result of lobe formation that is clustered in time.

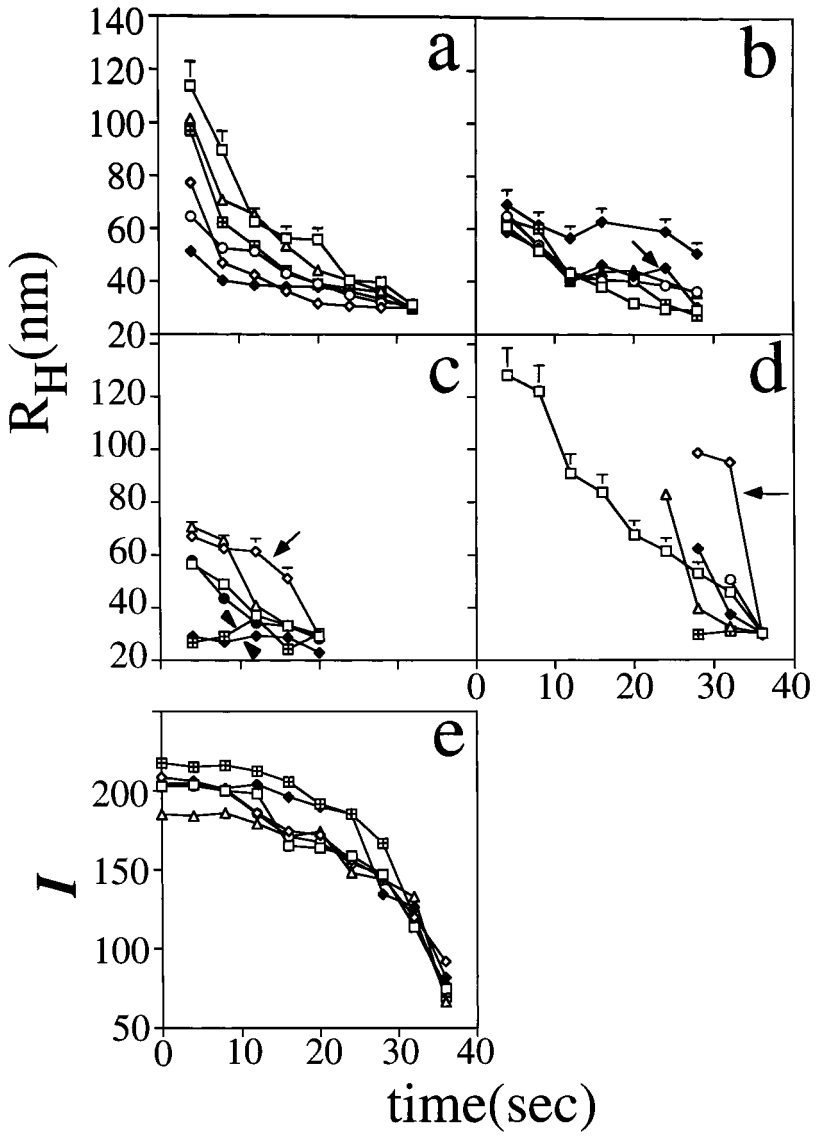

FIGURE 4 Quantitative analysis of DNA packaging-like events observed by light microscopy. The following are plotted as a function of time for DNA packaging-like events. (*a–c*) R_H for each lobe of three class 2 DNA molecules in a $T7_{3,5}$ DNA-metabolizing extract; (*d*) R_H for the class 2 DNA molecule imaged in Fig. 5 (low temperature preparation); (*e*) *I* for each lobe of a class 2 DNA molecule in a $T7_{3,5}$ extract. One-half the experimental error in R_H at any given time is indicated for all plots by a vertical bar in the uppermost plot of *a–d*. The time span of the plots varies for the following reasons: the time of the first data was limited, in all cases, by separation of lobes sufficient for tracking. In the case of *a–c* and *e*, the time of the first data was also limited by the time at which videotaping began. The class 2 DNA molecule used for (*a*) is also used for (*e*).

The comparatively small spread in time was consistently observed for the formation of high mobility fragments by type 2 DNA molecules. However, the following aspect of this process varied: although most R_H versus time plots had upward curvature (slope decreased in magnitude as time increased), some had regions with the opposite curvature (plots indicated by *arrows* in Fig. 4, *b* and *c*). Stalling-restarting of entry into a capsid is a possible explanation for the downward curvature.

The *I* value of a lobe progressively decreased during formation of a high mobility fragment. The ratio of initial *I*/final *I* was, on average, 2.8 ± 0.2. As expected, this ratio is equal to the ratio of *I* for unpackaged DNA/*I* for packaged DNA within experimental error. Qualitatively, the decrease in *I* is seen by inspection of both Fig. 3 and Fig. 5 (below). In contrast to the R_H versus time plots of Fig. 4 *a*, *I* versus time plots for the same type 2 DNA molecule have downward curvature (Fig. 4 *e*). This difference in curvature is expected for the following reasons: 1) the monomeric DNA packaged in bacteriophage T7 occupies one-half the volume of the cavity in which this DNA is packaged (Serwer, 1989). Thus, either decreased binding of DNA-specific dyes or fluorescence quenching is caused by steric constraint. In the case of ethidium, the existence of this constraint is confirmed by an increase in dye-mature bacteriophage binding that occurs when the DNA packaging density is decreased by deletion of DNA from the T7 genome (Griess et al., 1985). 2) Both the DNA packing density and the steric constraints will be comparatively small during the initial stage of DNA's entry into a capsid. Thus, DNA entry-associated decrease in *I* will also be comparatively small (possibly nonexistent) at this stage, even though R_H is decreasing. 3) As entry is completed, the decrease in *I* will become progressively steeper. The reason is that the DNA packing density increases; therefore, steric constraints accumulate. Thus, the plots in Fig. 4 confirm the following conclusion: the conversion of lobes to high mobility fragments is, at higher resolution, the packaging of concatemer-

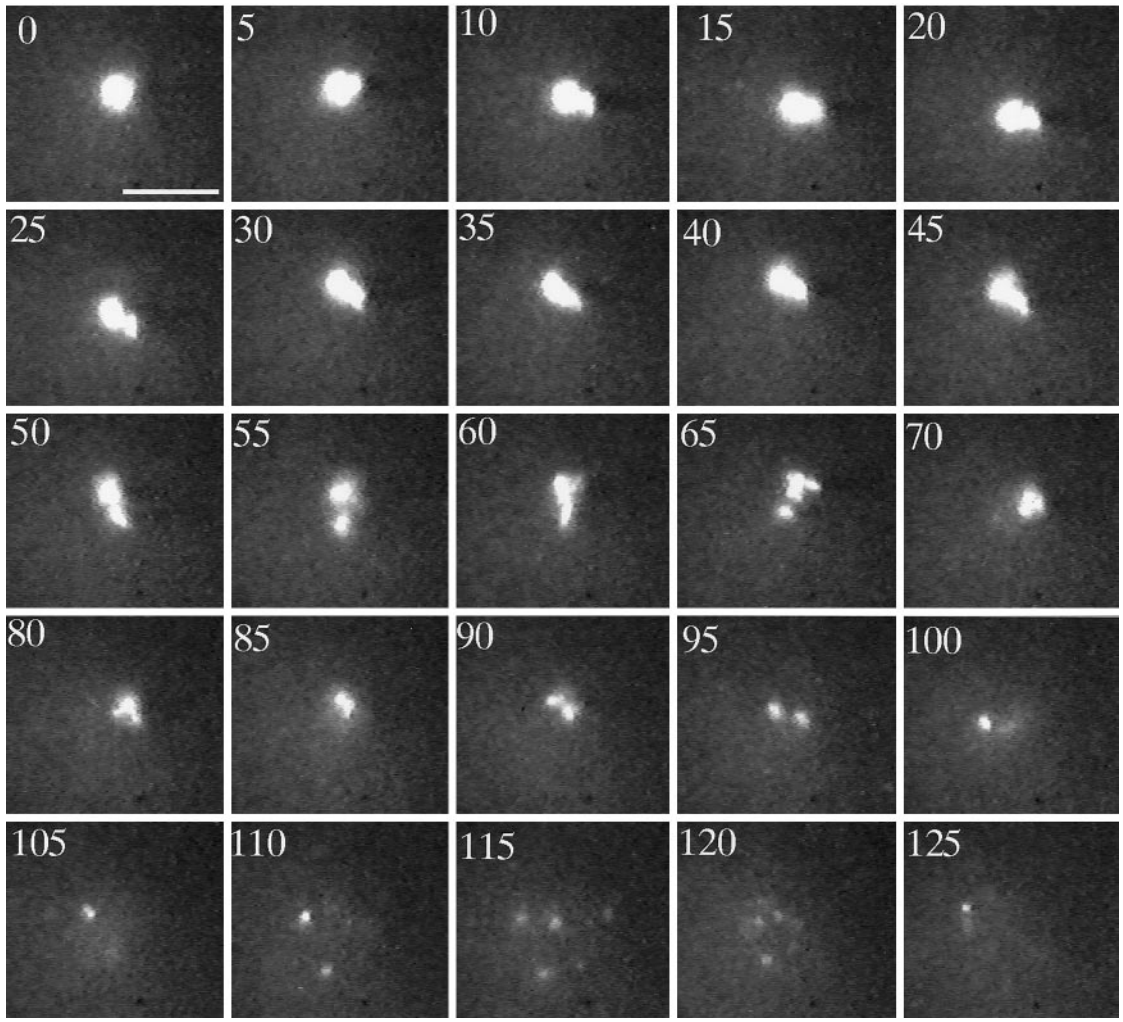

FIGURE 5 DNA packaging at lower temperature. DNA was added to a p6-supplemented $T7_{3,5,6}$ DNA-metabolizing extract. The low temperature procedure was used to both incubate and prepare a specimen for light microscopy. A class 2 DNA molecule is shown in the first frame. As described in the text, changes in this molecule are shown in subsequent frames. The length of the bar is 10 μm.

associated T7 genomes in bacteriophage capsids. This conclusion was originally based on the *R* and *I* values of the cleavage products, as well as the metabolism-dependence and the class 2 DNA-dependence of cleavage.

Improved visualization of the packaging of concatemer-associated T7 genomes

In an attempt to observe additional stages of DNA packaging, fluorescence microscopy was performed of DNA-extract mixtures that had been prepared by the low temperature procedure of the Materials and Methods section. In these mixtures, concatemerization at 0°C resulted in the formation of only a more limited version of the extensive fibrous DNA network that Sun et al. (1997) observed after concatemerization at 30°C (images not shown). Both the presence and the lobe formation of a class 2 DNA molecule were more detectable during scanning of the specimen. The frequency of lobe-forming class 2 DNA molecules was so low that it was not measured. However, occasionally a class 2 DNA molecule (class was judged by brightness) was observed that produced both lobes and, subsequently, high mobility fragments (Fig. 5). Unlike the class 2 DNA molecules in both Fig. 3 and Fig. 4, *a–c*, the class 2 DNA molecule in Fig. 5 was observed both before and during lobe formation. Initially (times between 0 and 45 s in Fig. 5; time (s) is indicated at the upper left), lobes were extruded. However, most lobes appeared to periodically retract. In most cases, a lobe could not be tracked as a separate entity. Subsequently (times between 45 and 60 s in Fig. 5), lobes became continuously established. Finally, the lobes converted to high mobility fragments (times between 60 and 125 s in Fig. 5).

R_H could not be determined for the high mobility fragments of Fig. 5 because the η of the DNA-metabolizing extract was not known. However, these fragments did undergo a roughly threefold decrease in *I* in comparison to their precursor-lobes. Assuming that the high mobility fragments of Fig. 5 were bacteriophage particles, η was determined from their Brownian motion (R_H assumed to be 30.1

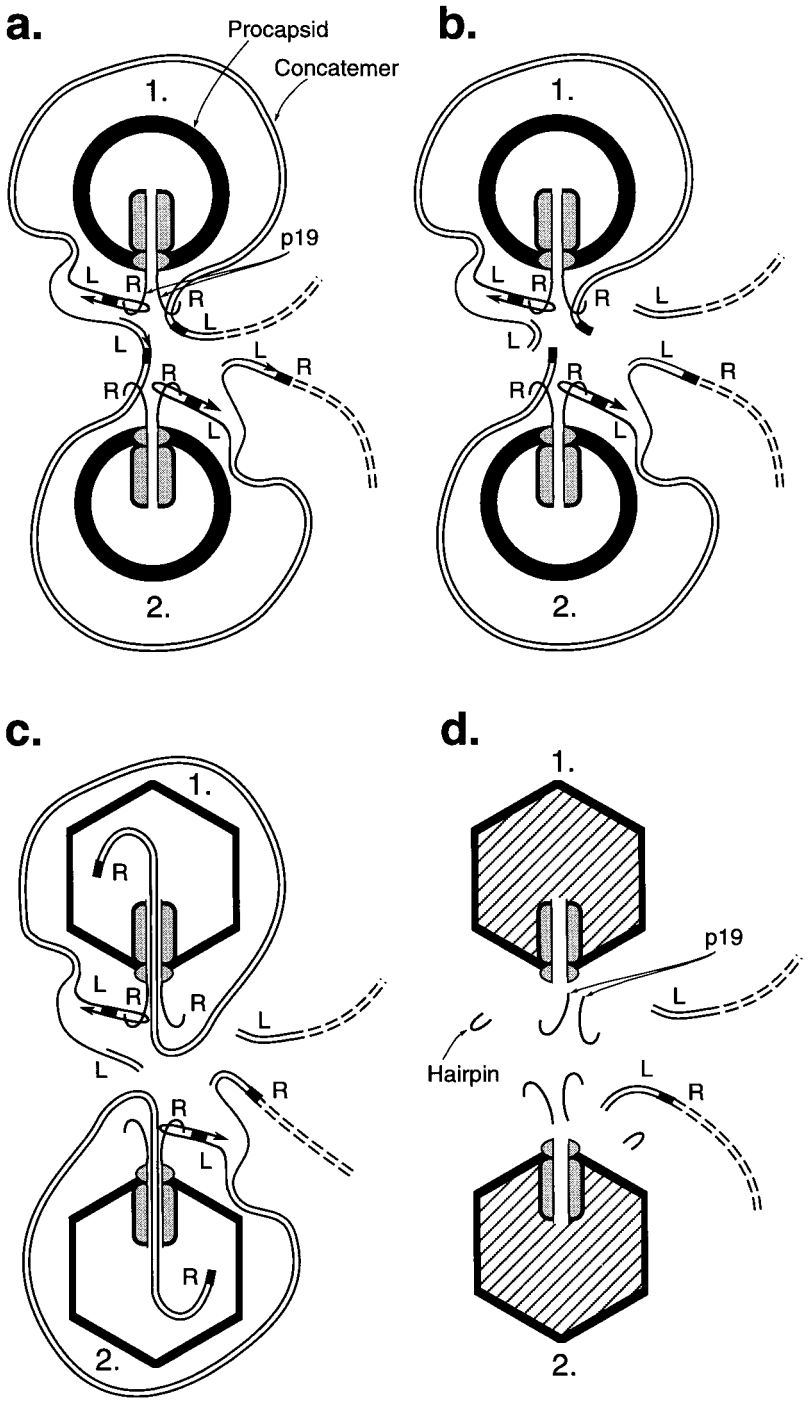

FIGURE 6 A hypothesized pathway that explains cooperativity during in vivo packaging of concatemer-associated T7 genomes. (*a*) A complex of a T7 concatemer and two procapsids (labeled *1* and *2*) is shown. Each procapsid binds the concatemer at two identical sites. Each site is a previously described Pac B site (Fujisawa and Hearing, 1994), one near the right end of each of two successive genomes in the concatemer. A hairpin-primed replicative branch duplicates the terminal repeat. The terminal repeat is indicated by filling the space between the two strands of a DNA double helix; an arrow within a DNA strand indicates replication of this strand. Each lobe observed by light microscopy corresponds to a capsid-associated loop of DNA drawn here. (*b*) After triggering that depends on formation of the complex in (*a*), the first of two cleavages occurs to initiate DNA packaging. (*c*) A freshly cleaved right end enters while the procapsid, capsid I, converts to the larger, more angular capsid, capsid II. (*d*) DNA both finishes entry and undergoes a terminal cleavage near the hairpin formed by replication. L, left; R, right end of a T7 genome. The initiating cleavage of at least the first genome shown in (*b*) has previously been found to occur (Sun et al., 1997) while the concatemer is part of a larger DNA network. In the figure, DNA network-associated initiating cleavages are not distinguished from initiating cleavages that occur after a concatemer is released from the DNA network. The events observed in Figs. 3–5 are both the entry of DNA and the terminating cleavage in (*c*) and (*d*). The complexes of Figs. 3–5 have additional capsids that, for simplicity, are not drawn here. In the pathway shown here, cleavage separates lobes before the separation is visible by light microscopy. In (*c*), end-first entry of DNA is drawn for simplicity. However, entry as a right end loop is equally compatible with the data. For visibility, the relative sizes of DNA, replicative branch, terminal repeat, and capsid have been altered.

nm; Eq. 1). The result was 2.1 cp, a reasonable value. Therefore, this η was used with Eq. 1 to determine R_H as a function of time, after continuous establishment of each lobe in Fig. 5. The results (Fig. 4 *d*) revealed a decrease in R_H for all lobes. However, only one lobe could be tracked from the time of its initial formation. The initial R_H of this lobe was larger than that of other lobes, but still 0.8 to 0.9 times the R_H of monomeric T7 DNA (Fig. 4 *d*). After becoming continuously established, the remaining lobes had R_H versus time plots (Fig. 4 *d*) that fell in the categories found for the R_H versus time plots in Fig. 4, *a*–*c*. One of the lobes had downward curvature even more dramatic than that of Fig. 4, *b* and *c* (*arrow* in Fig. 4 *d*).

DISCUSSION

Light microscopy has been used here to observe the metabolism of a single T7 concatemer to form viral particles. This observation appears to be the first observation of any complex DNA metabolism at the level of a single event. The observed DNA packaging events occurred in synchronized

clusters on type 2 DNA molecules. Synchronized clustering during in vitro T7 DNA packaging is explained by the hypothesis that cooperativity exists among the capsids that package the genomes of a single T7 concatemer. By this explanation, the cause of the five-lobe threshold is the comparative inefficiency of either four or fewer capsids in the cooperative initiation of DNA packaging. The threshold is determined by the comparatively poor environment, i.e., a DNA-metabolizing extract between a cover glass and a glass slide. Neither this nor any other threshold would necessarily exist inside a T7-infected cell.

In previous studies of bacteriophage DNA packaging, evidence has been presented that packaging of concatemer-associated genomes is processive. Processive packaging begins at the point of an initiating cleavage. The bacteriophages investigated in these previous studies include λ (Feiss, 1986), P22 (Casjens et al., 1992), SPP1 (Tavares et al., 1996), T1 (Hug et al., 1986) and T4 (Streisinger et al., 1967). In a further study of bacteriophage λ, genetic removal of an exonuclease of the bacterial host increases the efficiency with which monomeric (in contrast to concatemeric) DNA is packaged in vivo. Thus, the following conclusion has been drawn: avoidance of exonucleolytic genome damage is a reason for the evolution of a DNA packaging pathway in which concatemers are the primary substrates for DNA packaging (Thomason et al., 1997). If so, then the following question about processive packaging arises: how is a concatemer-associated genome protected from exonucleolytic damage after a neighboring genome is cleaved from the concatemer? A possible answer to this question is that the cooperativity observed for T7 also occurs for λ, P22, SPP1, T1, and T4. Cooperativity could occur during either DNA-capsid binding or a subsequent stage before processive initiating cleavages. By this hypothesis, cooperativity favors a delay in processive cleavages until genomes are protected by capsids. In the case of T7, the in vivo DNA packaging pathway of Fig. 6 is proposed here. In this pathway, cooperativity is achieved via interaction of capsid I particles bound to opposing branches produced during replication of the T7 terminal repeat. Evidence for the replicative branches is presented in Chung et al. (1990).

In theory, the rate of DNA entry into a capsid can be calculated from changes in R_H. In practice, uncertainty in the correlation of R_H with DNA packaged thwarts this calculation unless an assumption is made. The following assumption is made here: no DNA has been packaged for lobes that have the largest R_H values, 100–120 nm. If so, then the DNA enters a capsid at the average rate of 1 genome per 25–40 s (at 23°C) during the formation of high mobility fragments. In contrast to expectation, this rate is two to three times (significantly) higher than the rate previously measured (Son et al., 1993) for the average DNA that is packaged at 30°C in a mixture of a $T7_{4,9}$ and a $T7_{5,19}$ DNA-metabolizing extract. The reason for this phenomenon is not known. Determination of the kinetics of entry will require modification of the procedures used here.

The authors thank Dr. Gary A. Griess for assistance with procedures of digital image processing, Maree Hawks for a major effort in helping to determine R_H values, and Linda C. Winchester and Esther L. Hall for typing this manuscript.

The authors gratefully acknowledge support from the National Institutes of Health (GM24365) and the Welch Foundation (AQ-764).

REFERENCES

Bloomfield, V. A., D. M. Crothers, and I. Tinoco, Jr. 1974. Physical Chemistry of Nucleic Acids. Harper and Row, New York.

Bull, H. B. 1971. An Introduction to Physical Biochemistry. F. A. Davis Co., Philadelphia, PA.

Casjens, S. 1985. Nucleic acid packaging by viruses. *In* Virus Structure and Assembly. S. Casjens, editor. Jones and Bartlett, Boston, MA. 75–147.

Casjens, S., E. Wyckoff, M. Hayden, L. Sampson, K. Eppler, S. Randall, E. T. Moreno, and P. Serwer. 1992. Bacteriophage P22 portal protein is part of the gauge that regulates packing density of intravirion DNA. *J. Mol. Biol.* 224:1055–1074.

Chung, Y.-B., C. Nardone, and D. C. Hinkle. 1990. Bacteriophage T7 DNA packaging. III. A "hairpin end" formed on T7 concatemers may be an intermediate in the processing reaction. *J. Mol. Biol.* 216:939–948.

Dunn, J. J., and F. W. Studier. 1983. Complete nucleotide sequence of bacteriophage T7 DNA and the locations of T7 genetic elements. *J. Mol. Biol.* 166:477–535.

Feiss, M. 1986. Terminase and the recognition, cutting and packaging of λ chromosomes. *Trends Genet.* 2:100–104.

Fujisawa, H., and P. Hearing. 1994. Structure, function, packaging signals and specificity of the DNA in double-stranded DNA viruses. *Semin. Virol.* 5:5–13.

Griess, G. A., R. A. Harris, and P. Serwer. 1993. The trajectories of spheres during agarose gel electrophoresis. *Appl. Theor. Electrophor.* 3:305–315.

Griess, G. A., P. Serwer, and P. M. Horowitz. 1985. Binding of ethidium to bacteriophage T7 and T7 deletion mutants. *Biopolymers*. 24: 1635–1646.

Hug, H., R. Hausmann, J. Liebeschuetz, and D. A. Ritchie. 1986. In vitro packaging of foreign DNA into heads of bacteriophage T1. *J. Gen. Virol.* 67:333–343.

Kasas, S., N. H. Thomson, B. L. Smith, H. G. Hansma, X. Zhu, M. Guthold, C. Bustamante, E. T. Kool, M. Kashlev, and P. K. Hansma. 1997. *Escherichia coli* RNA polymerase activity observed using atomic force microscopy. *Biochemistry*.36:461–468.

Khan, S. A., S. J. Hayes, R. H. Watson, and P. Serwer. 1995. Specific, nonproductive cleavage of packaged bacteriophage T7 DNA in vivo. *Virology*. 10:409–420.

Perrin, J. 1913. Les Atomes. Alcan, Paris. Reprinted by Oxbow Press, Woodbridge, CT.

Schafer, D. A., J., Gelles, M. P. Sheetz, and R. Landick. 1991. Transcription by single molecules of RNA polymerase observed by light microscopy. *Nature*. 352:444–448.

Schwartz, D. C., X. Li, L. I. Hernandez, S. P. Ramnarain, E. J. Huff, and Y. K. Wang. 1993. Ordered restriction maps of *Saccharomyces cerevisiae* chromosomes constructed by optical mapping. *Science*. 262: 110–114.

Serwer, P. 1974. Fast sedimenting bacteriophage T7 DNA from T7-infected *Escherichia coli*. *Virology*. 59:70–88.

Serwer, P. 1989. Double-stranded DNA packaged in bacteriophages: conformation, energetics and packaging pathway. *In* Chromosomes: Eukaryotic, Prokaryotic and Viral, Vol. 3. K. W. Adolph, editor. CRC Press, Boca Raton, FL. 203–223.

Serwer, P., A. Estrada, and R. A. Harris. 1995. Video light microscopy of 670-kb DNA in a hanging drop: shape of the envelope of DNA. *Biophys. J.* 69:2649–2660.

Serwer, P., R. H. Watson, and S. J. Hayes. 1992. Formation of the right before the left mature DNA end during packaging-cleavage of bacteriophage T7 DNA concatemers. *J. Mol. Biol.* 226:311–317.

Smith, S. B., and A. J. Bendich. 1990. Electrophoretic charge density and persistence length of DNA as measured by fluorescence microscopy. *Biopolymers*. 29:1167–1173.

Smith, D. E., T. T. Perkins, and S. Chu. 1996. Dynamical scaling of DNA diffusion coefficients. *Macromolecules*. 29:1372–1373.

Son, M., S. J. Hayes, and P. Serwer. 1988. Concatemerization and packaging of bacteriophage T7 DNA in vitro: determination of the concatemers' length and appearance kinetics by use of rotating gel electrophoresis. *Virology*. 162:38–46.

Son, M., and P. Serwer. 1992. Role of exonuclease in the specificity of bacteriophage T7 DNA packaging. *Virology*. 190:824–833.

Son, M., R. H. Watson, and P. Serwer. 1993. The direction and rate of bacteriophage T7 DNA packaging in vitro. *Virology*. 196:282–289.

Steven, A. C., and B. L. Trus. 1986. The structure of bacteriophage T7. *In* Electron Microscopy of Proteins, Vol. 5. J. R. Harris and R. W. Horne, Editors. Academic Press, London. 1–35.

Streisinger, G., J. Emrich, and M. M. Stahl. 1967. Chromosome structure in phage T4. III. Terminal redundancy and length determination. *Proc. Natl. Acad. Sci. USA*. 57:292–295.

Stroud, R. M., P. Serwer, and M. J. Ross. 1981. Assembly of bacteriophage T7: dimensions of the bacteriophage and its capsids. *Biophys. J.* 36: 743–757.

Studier, F. W., and J. J. Dunn. 1983. Organization and expression of bacteriophage T7 DNA. *Cold Spring Harbor Symp. Quant. Biol.* 67: 999–1007.

Sun, M., M. Son, and P. Serwer. 1997. Formation and cleavage of a DNA network during in vitro bacteriophage T7 DNA packaging: light microscopy of DNA metabolism. *Biochemistry*. 36:13018–13026.

Takahashi, M., K. Yoshikawa, V. V. Vasilevskaya, and A. R. Khokhlov. 1997. Discrete coil-globule transition of single duplex DNAs induced by polyamines. *J. Phys. Chem. B.* 101:9396–9401.

Tavares, P., R. Lurz, A. Stiege, B. Rückert, and T. A. Trautner. 1996. Sequential headful packaging and the fate of the cleaved DNA ends in bacteriophage SPP1. *J. Mol. Biol.* 264:954–967.

Thomason, L. C., D. S. Thaler, M. M. Stahl, and F. W. Stahl. 1997. In vivo packaging of bacteriophage lambda monomeric chromosomes. *J. Mol. Biol.* 267:75–87.

Tinoco, I., Jr., K. Sauer, and J. C. Wang. 1995. Physical Chemistry: Principles and Applications in the Biological Sciences. Prentice Hall, Upper Saddle River, NJ.

White, J. H., and C. C. Richardson. 1987. Processing of concatemers of bacteriophage T7 DNA in vitro. *J. Biol Chem.* 262:8851–8860.

Yin, H., R. Landick, and J. Gelles. 1994. Tethered particle motion method for studying transcript elongation by a single RNA polymerase molecule. *Biophys. J.* 67:2468–2478.

Yin, H., M. D. Wang, K. Svoboda, R. Landick, S. M. Block, and J. Gelles. 1995. Transcription against an applied force. *Science*. 270:1653–1657.